Inorg. Chem. **2007**, *46*, 9463–9472

Structurally Diverse Aggregating Condensations of Ti(IV) Catecholates

Warren A. Wallace and Pierre G. Potvin*

Department of Chemistry, York University, 4700 Keele Street, Toronto, Ontario, Canada M3J 1P3

Received July 8, 2007

The simple 1:1 reaction of naphthalene-2,3-diol (H_2Np) with $Ti(O^iPr)_4$ has a complicated outcome, one rich in diversity and elucidated in this paper by X-ray crystallography and NMR spectroscopy. The reaction in $CDCl_3$ produces a crystalline precipitate, which was found to be the symmetrical dimer $[TiNp(O^iPr)_2]_2(HO^iPr)_2$ whose coordinated HO^iPr units are hydrogen bonded to O^iPr groups (**A**). A second crystal was also harvested and found to be a partially hydrolyzed 6:6 assembly $[Ti_3(\mu_3\text{-}O)(\mu\text{-}Np)_2(Np)(\mu\text{-}O^iPr)(O^iPr)(HO^iPr)_2(\mu\text{-}O)]_2$ (**B**) constructed of μ-oxo-linked inverted halves, each a 3:3 assembly anchored by a μ_3-oxo group. The supernatant was deduced to contain a soluble 3:3 product $[TiNp(O^iPr)_2]_3(HO^iPr)$ possessing the same stereochemistry as **B** and its likely hydrolysis precursor. When **A** was redissolved, it produced what appeared to be a 4:4 condensation product, which was also present in the supernatant when the reaction was conducted in the presence of HO^iPr-absorbing 13X molecular sieves, or when the reaction mixture was heated. In an analogous reaction, $Ti(O^tBu)_4$ produced only an **A**-like dimeric product possessing pentacoordinate metal centers.

Introduction

Some years ago, we investigated the stabilization of the fluxional tartrate ester complexes of Ti(IV) (Sharpless catalysts) by reaction with various bidentate ligands[1] and found that catechol and naphthalene-2,3-diol cleanly formed soluble, mixed-ligand products that appeared to be unsymmetrical dinuclear adducts. However, not being able to grow crystals, we could not ascertain their structures. We also found that these catechols alone engaged in rather complicated reactions with $Ti(O^iPr)_4$, again affording low-symmetry soluble products.

The interest in such species has in the meantime grown. Catechol groups have recently been used to graft Ru^{II} photosensitizers onto the TiO_2 surfaces of the photoelectrodes used in photovoltaic cells.[2] The grafting was reportedly faster and more efficient than with carboxylated sensitizers, presumably by reaction of the catechol moiety with the surface TiO_2. Indeed, the adsorption of catechol itself to particulate TiO_2 has been much studied of late;[3] catechol is thought to adsorb by coordination and hydrogen bonding and to chelate to the surface metals,[4] whence the chelated form sensitizes the surface to visible light, undergoes photoinduced electron release, and polymerizes to humic-like substances.[5]

Very recently, Davidson et al. reported the crystal structures of a number of catechol−$Ti(O^iPr)_4$ products and investigated their activities in ϵ-lactone ring-opening polymerization.[6] They also list some other applications of aryloxide complexes. In revisiting our earlier work, we chose to focus on naphthalene-2,3-diol because of its more easily understood ^{1}H NMR signals, and we report here on the rich coordination chemistry evident in its solid- and solution-state reaction products.

Results

The reaction of $Ti(O^iPr)_4$ with 1 equiv of naphthalene-2,3-diol (H_2Np) in $CDCl_3$ containing various amounts of molecular sieves produced a deep-red solution and a copious amount of lighter-colored solid. Dilution and heating resulted in the dissolution of much of the solid, and overlaying this with dry petroleum ether afforded diffraction-quality single crystals of two products. The supernatant was examined by

* To whom correspondence should be addressed. E-mail: pgpotvin@yorku.ca.

(1) Potvin, P. G.; Fieldhouse, B. G. *Can. J. Chem.* **1995**, *73*, 401−413.
(2) Rice, C. R.; Ward, M. D.; Nazeeruddin, M. K.; Grätzel, M. *New J. Chem.* **2000**, *24*, 651−652.
(3) Connor, P. A.; Dobson, K. D.; McQuillan, A. J. *Langmuir* **1995**, *11*, 4193−4195. Rodriguez, R.; Blesa, M. A.; Regazzoni, A. E. *J. Colloid Interface Sci.* **1996**, *177*, 122−131. Vasudevan, D.; Stone, A. T. *Environ. Sci. Technol.* **1996**, *30*, 1604−1613. Araujo, P. Z.; Morando, P. J.; Blesa, M. A. *Langmuir* **2005**, *21*, 3470−3474.
(4) Redfern, P. C.; Zapol, P.; Curtiss, L. A.; Rajh, T.; Thurnauer, M. C. *J. Phys. Chem. B* **2003**, *107*, 11419−11427.
(5) Lana-Villarreal, T.; Rodes, A.; Pérez, J. M.; Gómez, R. *J. Am. Chem. Soc.* **2005**, *127*, 12601−12611.
(6) Davidson, M. G.; Jones, M. D.; Lunn, M. D.; Mahon, M. F. *Inorg. Chem.* **2006**, *45*, 2282−2287.

10.1021/ic7013495 CCC: $37.00
Published on Web 09/29/2007

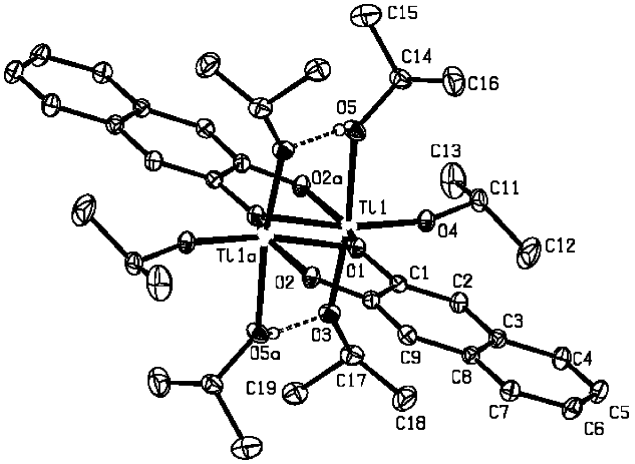

Figure 1. Crystal structure of [Ti*Np*(O^{i}Pr)$_2$]$_2$ (**A**), showing both crystallographic halves. Hydrogen atoms have been omitted for clarity, except that in the hydrogen bond between O(3) and O(5).

Table 1. Crystallographic Data[a]

	A	**B**
formula	$C_{38}H_{56}O_{10}Ti_2$	$C_{88}H_{100}Cl_{12}O_{24}Ti_6$
M	768.57	2254.48
space group	$P2_1/c$ (No. 14)	$P\bar{1}$ (No. 2)
a (Å)	9.1202(3)	12.6267(6)
b (Å)	13.2285(5)	13.4917(6)
c (Å)	16.8642(4)	15.6335(9)
α (deg)		95.798(3)
β (deg)	100.2920(19)	97.372(3)
γ (deg)		104.835(3)
V (Å^3)	2001.87(11)	2528.2(2)
Z	2	1
D_{calc} (g cm^{-3})	1.275	1.481
μ(Mo Kα) (mm^{-1})	0.451	0.837
$R(F_o)$	0.0453	0.0725
$R_w(F_o^2)$	0.1277	0.2215

[a] In both cases, $T = 150(1)$ K and $\lambda = 0.71073$ Å.

Table 2. Selected Bond Distances (Å) and Angles (deg) for **A**

Ti(1)−O(1)	2.0169(14)	Ti(1)−O(3)−C(17)	130.16(14)
Ti(1)−O(1a)	2.1079(15)	Ti(1)−O(4)−C(11)	161.00(14)
Ti(1)−O(2a)	1.9065(15)	Ti(1)−O(5)−C(14)	130.45(15)
Ti(1)−O(3)	1.8517(15)	O(3)−Ti(1)−O(5)	164.79(7)
Ti(1)−O(4)	1.7634(15)	O(5)−H(5O)	0.80(3)
Ti(1)−O(5)	2.1752(17)	H(5O)−O(3a)	1.99(3)
Ti(1)−Ti(1a)	3.3164(8)	O(5)−O(3a)	2.760(2)
		O(5)−H(5O)−O(3a)	162(3)

NMR techniques, and the main crystalline product could be redissolved in fresh solvent for NMR analysis.

Crystalline 2:2 Product. The more abundant, light-orange material was found to possess structure **A** (Figure 1 and Tables 1 and 2) of formula [Ti(*μ-Np*)(O^{i}Pr)$_2$(HO^{i}Pr)]$_2$, a dimeric complex formed from two equal halves related by an inversion center, whose Ti_2O_2 core was formed by nearly coplanar and bridging *Np* units (the parallel Ti*Np* planes were 0.52 Å apart). This quasi-planar core motif is analogous to the $M_2(\mu\text{-L})_2$ motifs found in the structures of the catechol analogues,[6] of [ZrCp$_2$(*μ*-Cat)]$_2$ (H$_2$Cat is catechol) described by Erker et al.,[7] and of [Ti(DTBC)(*μ*-DTBC)(HDTBC)]$_2^{2-}$ (H$_2$DTBC is 3,5-di-*tert*-butylcatechol) of Raymond et al.[8]

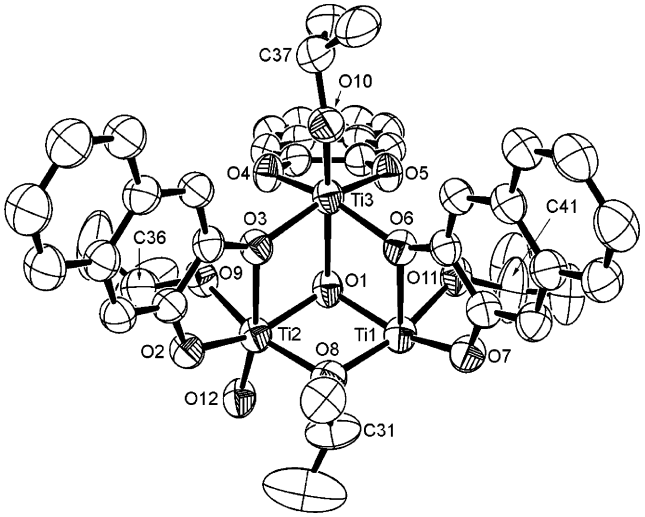

Figure 2. Crystallographically unique half of [Ti$_3$(*μ*$_3$-O)(*μ*-O)(*μ-Np*)$_2$(*Np*)-(*μ*-O^{i}Pr)(O^{i}Pr)(HO^{i}Pr)$_2$]$_2$ (**B**). Hydrogen atoms have been omitted for clarity. Hydrogen bonds (not depicted) were found between O(4) and O(9) and between O(11) and O(5).

With this core designating the equatorial plane, the remaining equatorial positions were occupied by O^{i}Pr ligands, in which *π* bonding to the metal was made evident by short Ti−O(4) bonds (1.763 Å) and obtuse Ti−O(4)−C(11) angles (169°). Such $Ti_2(\mu\text{-O})_2$ cores and *π*-bonded terminal alkoxides are commonly encountered.[6,9] The *π* donation was matched to longer trans-disposed bonds to the bridging *Np* oxygen (2.108 Å), relative to the shorter one to the nonbridging *Np* oxygen (1.906 Å). In contrast to the equatorial O^{i}Pr groups, the axial ligands showed longer Ti−O bonds and more acute Ti−O−C angles. These positions were occupied by a second type of O^{i}Pr group and by a coordinated HO^{i}Pr group, which was hydrogen bonded to the axial O^{i}Pr group lying syn to it on the other metal (the hydrogen bonding was confirmed by the location of the hydrogens employed), forming a Ti−O−H···O−Ti bridge. The Ti−O(3)−Ti−O(5) angle between axial ligands was pinched (to 164.8°) to achieve a favorable distance between the hydrogen-bonding partners (2.760 Å) and a more-favorable O−H−O angle (162.2°). Such pinched hydrogen-bond bridges had previously been found in several analogous structures.[6,10]

Crystalline 6:6 Product. The pale crystals of **A** were dotted with a small amount of darker-red crystals. One of these was harvested at the same time and found to exhibit structure **B** (Figure 2and Tables 1 and 3) of formula [Ti$_3$-(*μ*$_3$-O)(*μ*-O)(*μ-Np*)$_2$(*Np*)(*μ*-O^{i}Pr)(O^{i}Pr)(HO^{i}Pr)$_2$]$_2$. Like **A**, this assembly was also comprised of two equal halves related by inversion but linked through oxo bridges at O(12). Each

(7) Erker, G.; Noe, R. *J. Chem. Soc., Dalton Trans.* **1991**, 685−692.
(8) Borgias, B. A.; Cooper, S. R.; Bai Koh, Y.; Raymond, K. N. *Inorg. Chem.* **1984**, *23*, 1009−1016.
(9) Williams, I. D.; Pedersen, S. F.; Sharpless, K. B.; Lippard, S. J. *J. Am. Chem. Soc.* **1984**, *106*, 6430−6431. Pedersen, S. F.; Dewan, J. C.; Eckman, R. R.; Sharpless, K. B. *J. Am. Chem. Soc.* **1987**, *109*, 1279−1282.
(10) Svetich, G. W.; Voge, A. A. *Chem. Commun.* **1971**, 676−677. Vaid, T. P.; Tanski, J. M.; Pette, J. M.; Lobkovsky, E. B.; Wolczanski, P. T. *Inorg. Chem.* **1999**, *38*, 3394−3405. Wu, Y. T.; Ho, Y. C.; Lin, C. C.; Gau, H. M. *Inorg. Chem.* **1996**, *35*, 5948. Pandey, A.; Gupta, V. D.; Noth, H. *Eur. J. Inorg. Chem.* **2000**, 135. Zechmann, C. A.; Huffman, J. C.; Folting, K.; Caulton, K. G. *Inorg. Chem.* **1998**, *37*, 5856. Chuck, C. J.; Davidson, M. G.; Jones, M. D.; Kociok-Köhn, G.; Lunn, M. D.; Wu, S. *Inorg. Chem.* **2006**, *45*, 6595−6597.

Table 3. Selected Bond Distances (Å) and Angles (deg) for **B**

Ti(1)−O(1)	1.901(3)	Ti(1)−Ti(3)	3.2420(11)
Ti(2)−O(1)	1.907(3)	Ti(2)−Ti(3)	3.2422(11)
Ti(3)−O(1)	2.151(3)	Ti(1a)−O(12)−Ti(2)	157.01(18)
Ti(1)−O(8)	1.983(3)	C(34)−O(9)−Ti(2)	129.0(3)
Ti(2)−O(8)	1.978(3)	C(37)−O(10)−Ti(3)	150.8(3)
Ti(1)−O(6)	2.140(3)	C(41)−O(11)−Ti(1)	131.1(4)
Ti(3)−O(6)	1.987(3)	O(9)−H(9O)	0.846(10)
Ti(2)−O(3)	2.134(3)	H(9O)−O(4)	1.83(2)
Ti(3)−O(3)	1.983(3)	O(9)−O(4)	2.650(4)
Ti(2)−O(12)	1.808(3)	O(9)−H(9O)−O(4)	163(6)
Ti(1)−O(12a)	1.804(3)	O(11)−H(11O)	0.847(10)
Ti(1)−O(11)	2.086(3)	H(11O)−O(5)	1.87(3)
Ti(2)−O(9)	2.088(3)	O(11)−O(5)	2.650(4)
Ti(3)−O(10)	1.763(3)	O(11)−H(11O)−O(5)	153(6)
Ti(1)−Ti(2)	3.0038(10)		

crystallographically unique half was accompanied in the unit cell by two disordered $CHCl_3$ solvate molecules. The cluster has pseudo-meso stereochemistry, with a pseudo-mirror plane running through Ti(3), O(1), and O(8). At its core is a Ti_3O_3 ring in a cyclohexane-like chair conformation capped with a μ_3-oxo group, O(1), conferring the aspect of a "half-box". The Ti pairs were also bridged by two asymmetrically bound *Np* units and one O*i*Pr oxygen, O(8). The third *Np* unit was nonbridging and chelated to the titanium lying on the pseudo-mirror plane, Ti(3), which also held the lone terminal O*i*Pr group.

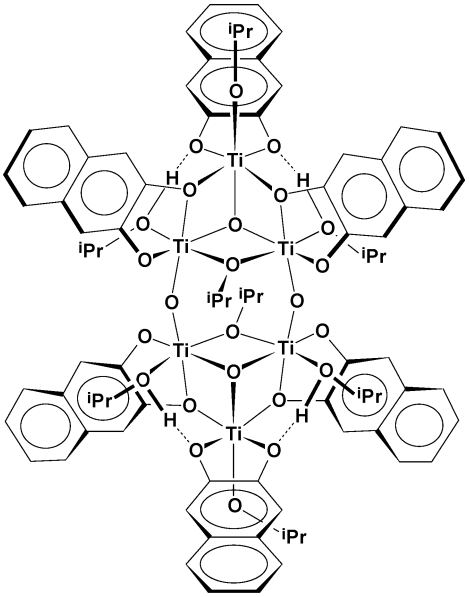

B

The oxygens of this third *Np* unit were hydrogen bonded on either side of the pseudo-mirror plane to a pair of HO*i*Pr molecules coordinated to the other two metals, as also confirmed by the location of the hydrogens involved. This hydrogen bonding pulled on and bent the *Np* unit 37.2° out of the O(3)−Ti(3)−O(6) plane, such that the coordination environment at Ti(3) was severely distorted from an ideal octahedron. Another view of the half-box is of three nearly orthogonal, edge-sharing, and flat rectangular Ti_2O_2 units (with angles of 102.9 ± 0.5° between least-squares planes). Whereas in **A**, the least-squares planes of the Ti*Np* unit and the Ti_2O_2 core were tilted 17.7° from each other, the μ-*Np* units in **B** were more perfectly coplanar with the Ti_2O_2 units to which they were fused (forming angles of 7.1° and 11.0° between least-squares planes).

There was evidence of π bonding by two O*i*Pr oxygens in **B**. First, the μ-O*i*Pr group defined a Ti_2O−C plane. Second, as with the equatorial O*i*Pr group of the 2:2 structure **A**, the lone terminal O*i*Pr group on the pseudo-mirror plane of **B** featured a short Ti(3)−O(10) bond (1.763 Å) and a large Ti(3)−O(10)−C(37) angle (150.8°). The trans Ti-μ_3-O bond was weak (2.151 Å), in comparison with the other two Ti-μ_3-O bonds (1.901 and 1.907 Å), either as a cause or a consequence of the π donation from O(10).

The half-box motif of **B** was also found in the quasi-C_3-symmetric and chiral $Ti_3(\mu_3\text{-O})(Cat)_4(HCat)_2\cdot 2py$[11] (py is pyridine), which can be written as the salt $(Hpy)_2[Ti_3(\mu_3\text{-O})(Cat)_6]$, and in the very close relative $[Ti_3(\mu_3\text{-O})(\mu\text{-O})(\mu\text{-O}^i\text{Pr})(O^i\text{Pr})(Cat)_2\{\mu\text{-}(CO)_9Co_3(\mu_3\text{-}CCO_2)\}_2]_2$ of the same, pseudo-meso stereochemistry, which is constructed, like **B**, of two equal, inverted halves in which the bridging *Np* units of **B** are replaced by bridging Cat units and where two bridging $Co(CO)_3$-substituted acetate groups replace the hydrogen-bonded *Np* and coordinated HO*i*Pr units.[12] In other instances, the box is closed by a second μ_3 group, for instance, an alkoxide.[13,14]

2:2 Product in Solution Phase. To perform NMR spectroscopy on product **A**, the bulk solid from an identical reaction mixture was isolated by decanting the supernatant, rinsing with petroleum ether, drying under a stream of Ar, then adding fresh $CDCl_3$. This produced spectra revealing signals from one principal component overlaid with lesser signals of minor components, which made precise signal integration difficult. The samples were apparently contaminated with some of the soluble supernatant material (vide infra) and/or with **B** and HO*i*Pr. The same spectral details also appeared when the original reaction was conducted in the presence of molecular sieves or when the reaction mixture was heated (vide infra). A complete analysis of the dominant species was thereby made possible with the aid of these other samples.

The ^{1}H NMR spectrum (Figure 3) was not consistent with structure **A** but clearly akin to it. As expected, it showed a single set of aromatic signals corresponding to an unsymmetrically bound *Np* unit. One *Np* singlet was far downfield of the other (both are labeled e) as befits a bridging unit, while the other was unusually *upfield* of the corresponding signal in free H_2*Np* (7.15 ppm), indicative of a moderately strong shielding effect at play, whereas no such effect was expected with **A**. There were two sharp O*i*Pr signals (labeled f and g) along with a larger, broader signal (labeled h) near 4.10 ppm, in a 2:1:∼5 ratio, whereas only two signals in 1:2 ratio were expected for **A**, assuming fast hydrogen

(11) Boyle, T. J.; Tribby, L. J.; Alam, T. M.; Bunge, S. D.; Holland, G. P. *Polyhedron* **2005**, *24*, 1143−1152.
(12) Lei, X.; Shang, M.; Fehlner, T. P. *Organometallics* **1997**, *16*, 5289−5301.
(13) Day, V. W.; Eberspacher, T. A.; Chen, Y.; Hao, J.; Klemperer, W. G. *Inorg. Chim. Acta* **1995**, *229*, 391−405.
(14) Steunou, N.; Ribot, F.; Boubekeur, K.; Maquet, J.; Sanchez, C. *New J. Chem.* **1999**, *23*, 1079−1086.

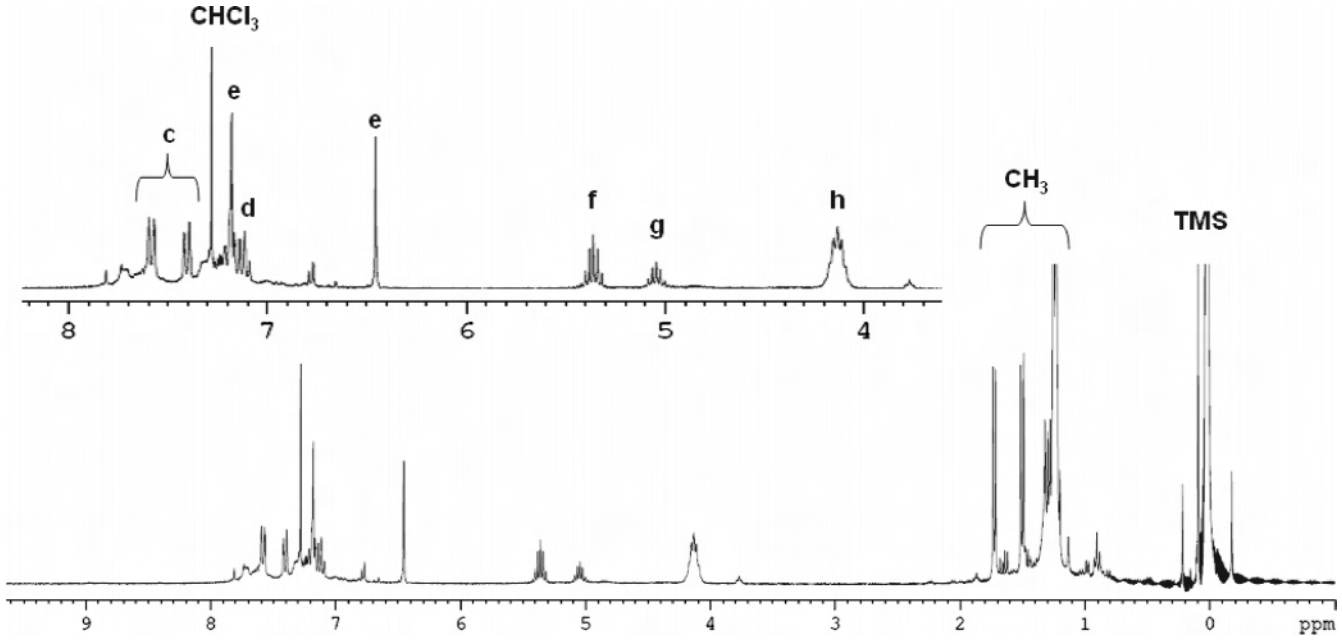

Figure 3. ^{1}H NMR spectrum of crystalline **A** redissolved in $CDCl_3$.

exchange between the hydrogen-bonded axial O^{i}Pr groups. The larger signal h must have involved free HO^{i}Pr, though it lay slightly downfield (4.10 ppm) of the signal for pure HO^{i}Pr (4.01 ppm). The same f and g signals appeared consistently in the same 2:1 ratio in other preparations as well, and so were not due to contamination, and the samples always contained HO^{i}Pr, though none was a priori expected. On the basis of an **A**-like Ti_2Np_2 structure, the sharp O^{i}Pr signals accounted for only three of the mandatory four O^{i}Pr groups. The larger signal was then evidently a coalesced signal reflecting an exchange between free HO^{i}Pr and the fourth TiO^{i}Pr group. This was corroborated by the appearance in the ^{13}C NMR spectrum of sharp OCH peaks near 84 and 79 ppm, also in 2:1 intensity ratio, and of a broad signal near 70 ppm, downfield of the signal from free HO^{i}Pr (63.9 ppm) and clearly also a coalesced signal. Correlation spectroscopy (COSY) showed that both sharp ^{1}H heptets were each associated with a pair of CH_3 doublets, indicating diastereotopicity.

These observations best fit a 4:4 species **C** (Chart 1) arising from the face-to-face, condensing "dimerization" of two molecules of **A**, with ejection of a HO^{i}Pr ligand from each "monomer", according to

$$2\mathbf{A} \rightleftarrows \mathbf{C} + 2\mathrm{HO}^i\mathrm{Pr} \qquad (1)$$

A similar dimerization in a solution of 2:4 titanium−tartrate ester assemblies had been seen in earlier work.[15] The chiral dimer **C** has diastereotopic O^{i}Pr bridges, as observed, whereas the CH_3 groups of the O^{i}Pr bridges in the meso isomer **C′** are related by mirror symmetry. Moreover, as indicated on the drawing of **C**, one of the two naphthalene H-1 atoms lies above (or below) a *Np* group, thereby accounting for the observed upfield position of one of the two *Np* singlets, whereas there would be no satisfactory origin of this shift in **C′**. Furthermore, because the Ti−O^{i}Pr−Ti linkage in **C** resembles the Ti−O−Ti linkage in **B**,

Chart 1. Isomeric Dimers of **A**, with Stereochemical and Shielding Differences[a]

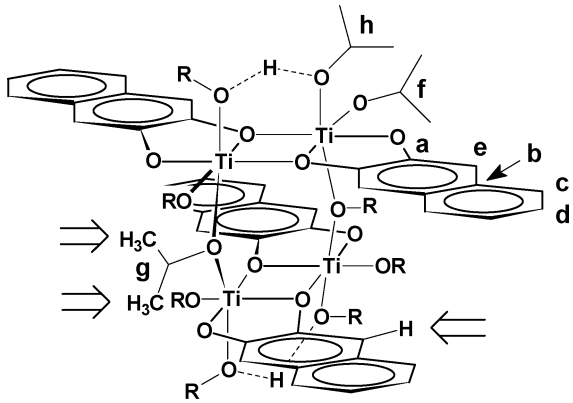

C R = ^{i}Pr

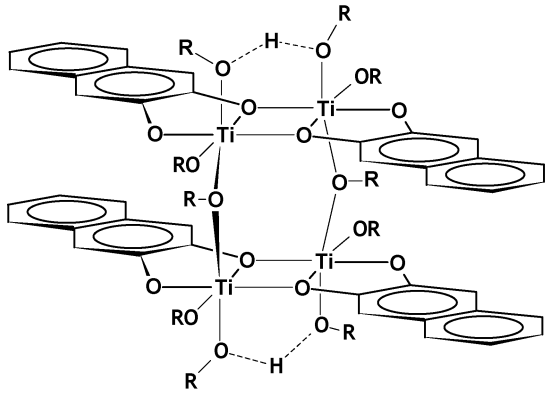

C′ R = ^{i}Pr

[a] Letters give the assignments of Figure 3. The arrows indicate diastereotopic CH_3 groups and a shielded ^{1}H nucleus.

(15) Potvin, P. G.; Fieldhouse, B. G. *Tetrahedron: Asymmetry* **1999**, *10*, 1661−1672.

the spacing between **A** subunits in **C** can be approximated by the Ti(1)···Ti(2′) spacing in **B** (3.54 Å). This spacing and the offset between stacked *Np* units in **C** is very propitious for stabilizing π-stacking interactions.[16]

As the redissolved form of the solid product is here deduced to result from an aggregation, whereas aggregation more frequently results in precipitation, we verified through elemental analysis that the isolated crystalline **A** and the bulk solid were indeed one and the same and that the crystal had not been fortuitously picked from a bulk material of different composition. This analysis revealed a slightly depressed percentage of carbon attributable to slight hydrolysis or to incomplete combustion of the aromatic carbons, but was otherwise consistent (C/H ratio 0.676) with the formulation of the bulk solid as **A** (C/H ratio 0.679). Importantly, it was not consistent with the bulk solid being a more highly condensed material such as **C** (C/H ≥ 0.729).

In respect to the observed integration ratio, the most downfield O^{i}Pr signal f was assigned to the four equatorial O^{i}Pr groups, the smaller ones g to the two bridging O^{i}Pr, and the remaining axial hydrogen-bonded ^{i}PrO−H−O^{i}Pr pairs seemed to engage in fast exchange with free HO^{i}Pr to give rise to the coalesced ^{1}H and ^{13}C signals h. With knowledge of the amount of free HO^{i}Pr contributing to the coalesced signal after subtracting the contribution from the ^{i}PrO−H−O^{i}Pr pairs, the position of the coalesced signal implied that the average chemical shift of the OCH signals from the ^{i}PrO−H−O^{i}Pr pairs was 4.32 ppm. This relatively upfield position for an O^{i}Pr methine signal can be explained by weaker Ti−O bonds to the hydrogen-bonded ^{i}PrO−H−O^{i}Pr oxygens. Indeed, the corresponding bonds in **A** averaged 2.014 Å in length, while those to the coordinated HO^{i}Pr in **B** averaged 2.082 Å, in comparison to an average 1.763 Å for bonds to terminal O^{i}Pr groups in both **A** and **B**. Campbell et al. found that [Ti(*m*-OC$_6$F$_5$)(OC$_6$F$_5$)$_2$(O^{i}Pr)(HO^{i}Pr)]$_2$ showed a coalesced signal for both O^{i}Pr and coordinated HO^{i}Pr groups (even though these were not hydrogen bonded) at 4.48 ppm, with an average Ti−O bond length of 1.921 Å.[17] They also report shifts ranging from 4.10 to 5.19 ppm (in C$_6$D$_6$) for the OCH signals from coordinated HO^{i}Pr units in three complexes of Ti(OR)$_4$(HO^{i}Pr) formed with variously fluorinated phenols.

Because bridging oxygens are expected to be more electron poor than terminal ones, the assignment of the more upfield O^{i}Pr methine signal to the most electron-poor O^{i}Pr group is counterintuitive. Senouci et al. had also found that μ-O^{i}Pr signals were upfield of those from terminal O^{i}Pr groups and gave as dividing lines 4.60 ppm for methine signals and 1.30 ppm for the methyl signals.[18] On the other hand, μ-O^{i}Pr groups are associated with longer Ti−O bonds, and Figure 4 relates the relation between the methine H chemical shifts and the corresponding Ti−O^{i}Pr bond-lengths, from those literature instances where both kinds of data are available.

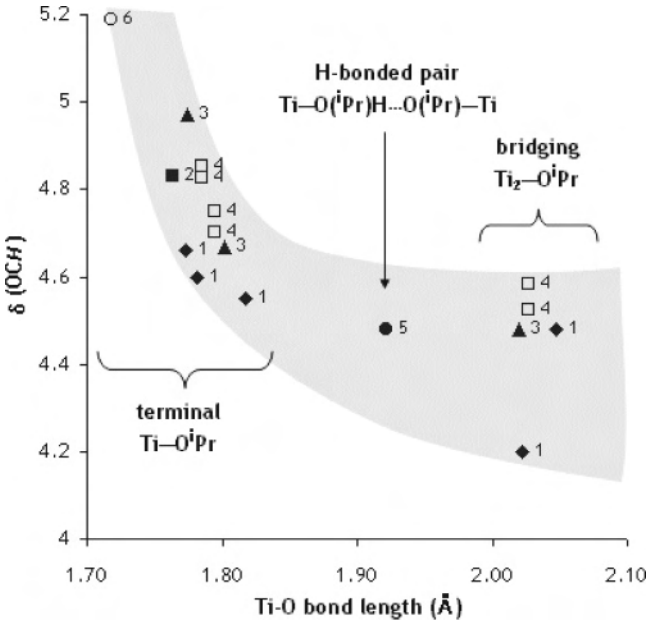

Figure 4. Plot of methine H chemical shifts against the corresponding unique or average Ti−O bond lengths of Ti−O^{i}Pr groups. The data points are labeled according to source, as follows: (1) Ti$_3$(O)(OOCCPh$_3$)$_2$(O^{i}Pr)$_8$ in CDCl$_3$ from Senouci et al.,[18] (2) [Ti$_3$(O)$_2$(O^{i}Pr)$_2$(Cat)$_2${(CO)$_9$Co$_3$(μ_3-CCO$_2$)}$_2$]$_2$ in C$_6$D$_6$ from Fehlner et al.,[12] (3) Ti$_3$O(O^{i}Pr)$_9$(OMe) in methylcyclohexane-d_{14} from Day et al.,[13] (4) Ti$_3$O(O^{i}Pr)$_7$(O$_3$C$_9$H$_{15}$) in C$_6$D$_6$ from Steunou et al.[14] and in CDCl$_3$ from Senouci et al.,[18] and (5) Ti(OC$_6$F$_5$)$_3$(O^{i}Pr)(HO^{i}Pr) and (6) Ti(O-2,6-F$_2$C$_6$H$_3$)$_3$(O^{i}Pr)$_3$ in C$_6$D$_6$ from Campbell et al.[17]

We find that these instances indeed fall in a band of values indicative of an inverse relationship that is useful for structural assignment, but we also find that values near 4.6 ppm do not allow for an unambiguous assignment. (Unfortunately, there are too few available ^{13}C NMR data with which to draw further correlations.) The assignments of our signals f and h as originating from terminal and bridging O^{i}Pr groups, respectively, are consistent with this correlation. Signal g appears more downfield than expected for a bridging O^{i}Pr group, but anisotropic effects from our *Np* units may be responsible.

Soluble 3:3 Product. The interesting 6:6 species **B** was obviously a product of partial hydrolysis by adventitious water, but it was not evident how it could have arisen from the 2:2 complex **A**, especially because the Ti$_2$*Np*$_2$ unit in **A** was expected to be endowed with pronounced stability, owing to extended conjugation. We therefore also examined the strongly colored supernatant of the initial reaction mixture, by laser desorption/ionization−time-of-flight (LDI-TOF) mass spectrometry and NMR spectroscopy.

The NMR spectra and their analyses were complex. Only salient points are presented here, with more detailed analysis found in the Supporting Information. There were three *Np* ^{1}H singlets in a 1:1:1 integration ratio (labeled e in Figure 5), and the aromatic ^{13}C NMR signals also occurred in groups of three peaks of equal intensity. These data indicated the presence of three *Np* units on three Ti centers, two of which are equivalent but unsymmetrical, while the third is symmetrical. One of the *Np* ^{1}H singlets was over 1 ppm downfield of the other two, and this pattern was echoed in the ^{13}C clusters a, b, and e as well. This phenomenon had

(16) Hunter, C. A.; Sanders, J. K. M. *J. Am. Chem. Soc.* **1990**, *112*, 5525−5534.
(17) Campbell, C.; Bott, S. G.; Larsen, R.; Van Der Sluys, W. G. *Inorg. Chem.* **1994**, *33*, 4950−4958.
(18) Senouci, A.; Yaakoub, M.; Huguenard, C.; Henry, M. *J. Mater. Chem.* **2004**, *14*, 3215−3230.

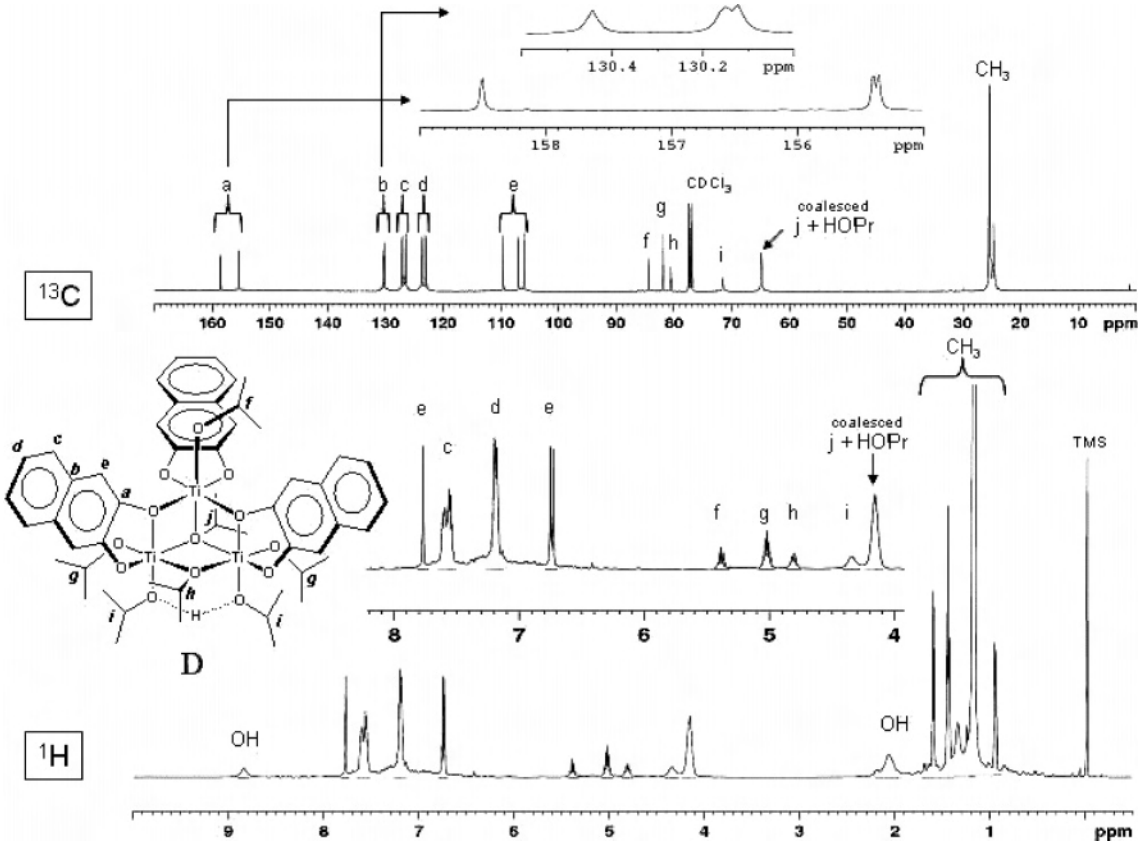

Figure 5. NMR spectra in $CDCl_3$ of the soluble reaction product, showing signal assignments. For greater clarity, the ^1H NMR spectrum displayed is that from a sample obtained in the presence of 1 g of molecular sieves, while that obtained without molecular sieves appears in the Supporting Information.

been evident with **C** and is attributed in the present case to one of the three kinds of *Np* oxygens serving as a bridge between two metals, as occurred in **A**−**C**.

There were five TiO^iPr/HO^iPr methine ^1H signals (f−j) in a 1:2:1:2:∼13 integration ratio and five corresponding ^{13}C signals. The largest and most upfield in each case (j) were due to HO^iPr liberated in the formation of both the solid (**A**) and the soluble product, but as in the case of **C**, they lay a little downfield of the corresponding signals from pure HO^iPr, indicating a coalescence phenomenon here as well. The relative integration of the ^1H NMR signal varied with temperature and with the presence of molecular sieves (vide infra). The first three O^{i}Pr ^1H signals (f−h) were sharp and correlated to three sharp ^{13}C signals, which were also in a ca. 1:2:1 intensity ratio. In contrast, the two most upfield ^1H signals (i and j) were shapeless and broad and failed to show $^1H-^{13}C$ correlations but were taken to be paired to the two broad ^{13}C signals lying upfield of the $CDCl_3$ signal. We could ascertain that signals i could not be due to unreacted Ti$(O^i$Pr$)_4$ (^1H at 4.49 ppm and ^{13}C at 76.2 ppm) in rapid exchange with HO^iPr, since Ti$(O^i$Pr$)_4-$HO^iPr exchanges are not fast enough in $CDCl_3$ at room temperature to generate a coalesced signal[19] and because we cannot have two simultaneous coalescence phenomena involving a common partner (free HO^iPr) giving two signals. Since the first four OCH signals (f−i) accounted for the six O^{i}Pr groups that suffice for an electroneutral Ti_3Np_3 cluster, and the fifth signal evidently included at least a seventh O^{i}Pr group, the complex necessarily included at least one coordinated HO^{i}Pr. This was supported by the observation of a 1H OH signal at 8.85 ppm. The signals labeled i could therefore be assigned to a hydrogen-bonded ^{i}PrO−HO^{i}Pr pair, exchanging quickly between each other but more slowly with free HO^{i}Pr, and the chemical shifts in both ^1H and ^{13}C NMR spectra were almost the same as those observed for the analogous ^{i}PrO−H−O^{i}Pr pair in **C**. These assignments were supported by COSY spectroscopy, which showed correlations to diastereotopic CH_3 signals for the 2H heptet g and not for the 1H heptets f and h. The CH_3 signals correlating to the other 2H methine signal i, which might also have revealed diastereotopicity, and to the coalesced signal j overlapped.

These findings were therefore consistent with a 3:3 structure of formula [Ti*Np*$(O^i$Pr$)_2]_3$(HO^{i}Pr). Structure **D** (Figure 5) is one of five stereoisomers of this formula possessing the symmetry required by NMR. Only one other isomer has bridging *Np* units, but its bridging *Np* oxygens are pyramidalized (the Ti−O−Ti fragments are bent); resonance and conjugation are thereby impeded, and this alternative must be less stable. Indeed, Zerner's intermediate neglect of differential overlap (ZINDO/1) calculations confirmed that **D** is the most stable of all five of these isomers.

The measured integration ratios of the ^1H signals implied a ca. 7:2 ratio of **A** and **D** products, as in

(19) Potvin, P. G.; Gau, R.; Kwong, P. C. C.; Bianchet, S. *Can. J. Chem.* **1989**, *67*, 1523−1537.

$$20\mathrm{Ti(O^{\mathit{i}}Pr)_4} + 20\mathrm{H_2}\mathit{Np} \rightarrow 7[\mathrm{Ti}\mathit{Np}(\mathrm{O^{\mathit{i}}Pr})_2]_2(\mathrm{HO^{\mathit{i}}Pr})_2\ (\mathbf{A}) + 2[\mathrm{Ti}\mathit{Np}(\mathrm{O^{\mathit{i}}Pr})_2]_3(\mathrm{HO^{\mathit{i}}Pr})\ (\mathbf{D}) + 24\mathrm{HO^{\mathit{i}}Pr} \quad (2)$$

Structure **D** has the same architecture and stereochemistry as the crystallographically unique half of **B** described earlier and is therefore the likely source of **B** through partial hydrolysis (eq 3), with the probable replacement of the most labile groups.

$$2[\mathrm{Ti}\mathit{Np}(\mathrm{O^{\mathit{i}}Pr})_2]_3(\mathrm{HO^{\mathit{i}}Pr})\ (\mathbf{D}) + 4\mathrm{H_2O} \rightarrow \mathrm{Ti_6}\mathit{Np}_6\mathrm{O_4(O^{\mathit{i}}Pr)_4(HO^{\mathit{i}}Pr)_4}\ (\mathbf{B}) + 6\mathrm{HO^{\mathit{i}}Pr} \quad (3)$$

D differs from **B** in that, without divalent oxo bridges, it includes only one molecule of coordinated HO*i*Pr, compared to two in each 3:3 half of **B**, and so it cannot employ the same hydrogen-bonding scheme. Instead, **D** has a hydrogen-bonded *i*PrO−H−O*i*Pr pair spanning a Ti_2O_2 ring, exactly as that occurring in the 2:2 complex **A**. As a result, the symmetrical *Np* unit can assume a more normal disposition, in contrast to the effect of the lateral hydrogen bonding in **B**.

A unique feature of **D** is the triply bridging O*i*Pr group (labeled j in Figure 5). Although less common than μ-O*i*Pr groups, there are many literature examples of μ_3-O*i*Pr groups, having been detected in crystals of a Mo complex,[20] in clusters containing M_2Ti (M = Sr,[21] Tl,[22] Ce,[23] Pb,[24,25] Cd,[26] Li,[27] Ba[28]) or MTi_2 (M = Fe,[29] Ba,[30] Y,[30] Cu,[30] Pb,[31] Sn[31,32]) as well as $CdSn_2$,[31] $PbZr_2$,[31] and $SnZr_2$.[31,32] They have also been found in $[Ti_3(\mu_3\text{-O}^{\mathit{i}}\mathrm{Pr})_2(\mu\text{-O}^{\mathit{i}}\mathrm{Pr})_3(\mathrm{O}^{\mathit{i}}\mathrm{Pr})_6]^+$ salts[32,33] and identified in solution by NMR in the partly hydrolyzed $Ti_3O(O^{\mathit{i}}Pr)_{10}$.[13] Even with the help of the lateral hydrogen bonding, the related μ_3-O group of **B** made the weakest Ti−O bonds in that structure—the weakest of all, Ti(3)−O(1), was to the mirror-plane Ti, and it was about 0.4 Å longer than the shortest Ti−O bond. A μ_3-O*i*Pr group in the corresponding position in **D** would therefore be expected to generate steric stress, a stress that its replacement during partial hydrolysis to **B** would relieve. A weakening of Ti−O bonds owing to this stress would add lability. The product assigned structure **D** was indeed fragile: the LDI-TOF mass spectra displayed only uninformative fragments of low mass, and its NMR signals disappeared in the presence of large amounts of molecular sieves (vide infra) or excess H_2Np, having been replaced by very broad and featureless signals bearing no evident relation to those of **D**. Such lability would also be consistent with the observed fast exchange with free HO*i*Pr, since the dissociation of a weakened Ti−O bond would facilitate the exchange. It is therefore reasonable to assign the coalesced signals j to the μ_3-O*i*Pr group in **D**.

With the exception of signal h, which was further downfield than expected, the O*i*Pr methine ^{1}H signal assignments (Figure 5) were consistent with the correlation of Figure 4. Signal h, like signal g in Figure 3, appears more downfield than this correlation would predict, perhaps because of the *Np* magnetic anisotropy.

We attempted ^{1}H NMR spectroscopy at lower temperatures to slow the exchanges, but this was inconclusive: we witnessed generalized signal broadening, complicated by a downfield migration of the HO*i*Pr OH signal to obscure the methine region, with no detectable resolution of the coalesced peak j. We also attempted to isolate this product free from HO*i*Pr. Even with large proportions of petroleum ether, precipitation was slow and incomplete. This or simple evaporation produced amorphous material that failed to redissolve.

Effects of Molecular Sieves or Heating. When 1:1 reaction mixtures of $Ti(O^{\mathit{i}}Pr)_4$ and H_2Np, containing both solid (**A**) and supernatant (**D**), were heated to 53−59 °C, much of the precipitate **A** dissolved, and the NMR spectra clearly showed, alongside the previously observed signals for **D**, the presence of the same signals earlier attributed to the 4:4 complex **C**. At the same time, the relative amount of HO*i*Pr present increased, and the coalesced signal j migrated downfield slightly while signal i disappeared entirely, indicating that both i and j were now coalescing together. Cooling the solution back to room temperature restored the original spectra, as the precipitate re-formed.

The presence of powdered 13X molecular sieves had a related effect: with increasing amounts of sieves present, the amount of free HO*i*Pr progressively dropped, while the signal j migrated downfield to overtake signal i, and signals from **C** became more and more apparent. With 4 g of sieves present, there were no signals i and j in evidence, the remaining signals from **D** had broadened and become completely indistinct, and the only sharp signals present were those from **C**. This allowed clear detection of the diastereotopic CH_3 signals.

Clearly, the removal of the free HO*i*Pr with sieves had caused a shift of the **A** ↔ **C** equilibrium (eq 1), converting the insoluble **A** to the soluble **C** with an entropically driven release of additional HO*i*Pr, while heating had caused the same shift. Because independent samples of **D** and **C** alone

(20) Chisholm, M. H.; Folting, K.; Huffman, J. C.; Kirkpatrick, C. C. *Inorg. Chem.* **1984**, *23*, 1021. Chisholm, M. H.; Folting, K.; Huffman, J. C.; Kirkpatrick, C. C. *J. Am. Chem. Soc.* **1981**, *103*, 5967.

(21) Baxter, I.; Drake, S. R.; Hursthouse, M. B.; Malik, K. M. A.; Mingos, D. M. P.; Plakatouras, J. C.; Otway, D. J. *Polyhedron* **1998**, *17*, 625−639.

(22) Boyle, T. J.; Zechmann, C. A.; Alam, T. M.; Rodriguez, M. A.; Hijar, C. A.; Scott, B. L. *Inorg. Chem.* **2002**, *41*, 946−957.

(23) Hubert-Pfalzgraf, L. G.; Abada, V.; Vaissermann, J. *Polyhedron* **1999**, *18*, 3497−3504.

(24) Hubert-Pfalzgraf, L. G.; Daniele, S.; Papiernik, R.; Massiani, M.-C.; Septe, B.; Vaissermann, J.; Daran, J.-C. *J. Mater. Chem.* **1997**, *7*, 753−762.

(25) Daniele, S.; Papiernik, R.; Hubert-Pfalzgraf, L. G.; Jagner, S.; Hakansson, M. *Inorg. Chem.* **1995**, *34*, 628−32.

(26) Veith, M.; Mathur, S.; Huch, V. *Inorg. Chem.* **1996**, *35*, 7295−7303.

(27) Kuhlman, R.; Vaartstra, B. A.; Streib, W. E.; Huffman, J. C.; Caulton, K. G. *Inorg. Chem.* **1993**, *32*, 1272−8.

(28) Yanovskii, A. I.; Yanovskaya, M. I.; Limar, V. K.; Kessler, V. G.; Turova, N. Ya.; Struchkov, Yu. T. *J. Chem. Soc., Chem. Commun.* **1991**, 1605−6.

(29) Nunes, G. G.; Reis, D. M.; Amorim, P. T.; Sa, E. L.; Mangrich, A. S.; Evans, D. J.; Hitchcock, P. B.; Leigh, G. J.; Nunes, F. S.; Soares, J. F. *New J. Chem.* **2002**, *26*, 519−522.

(30) Veith, M.; Mathur, S.; Huch, V. *Inorg. Chem.* **1997**, *36*, 2391−2399.

(31) Veith, M.; Mathur, S.; Huch, V. *J. Chem. Soc., Dalton Trans.* **1996**, 2485−2490.

(32) Veith, M.; Mathur, S.; Huch, V. *J. Chem Soc., Chem. Commun.* **1997**, 2197−2198.

(33) Reis, D. M.; Nunes, G. G.; Sa, E. L.; Friedermann, G. R.; Mangrich, A. S.; Evans, D. J.; Hitchcock, P. B.; Leigh, G. J.; Soares, J. F. *New J. Chem.* **2004**, *28*, 1168−1176.

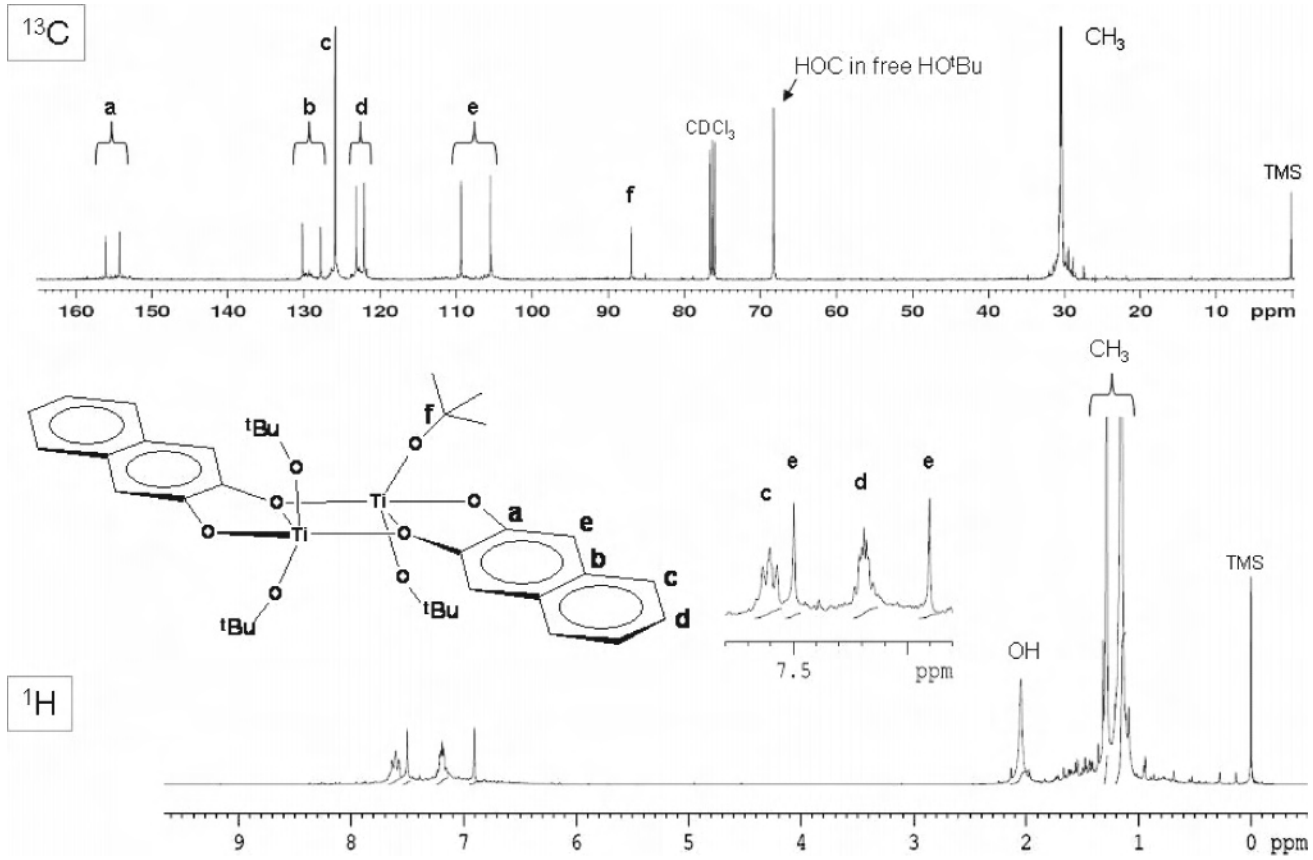

Figure 6. NMR spectra, with signal assignments, of the Ti(O^{t}Bu)$_4$ reaction product, assigned structure **E**.

could be generated, products **C** and **D** were evidently not in equilibrium. Hence, **A** and **D** were not in equilibrium either, since our experiments showed that **A** and **C** were interconvertible through heating or by depletion of HO^{i}Pr.

Reaction with Ti(O^{t}Bu)$_4$. We also examined the reaction of Ti(O^{t}Bu)$_4$ with 1 equiv of H$_2$*Np* in $CDCl_3$. The material was not fully characterized, but the solution NMR spectra were entirely consistent with the 2:2 adduct **E** (Figure 6), in particular showing five groups of paired aromatic signals very similar to those of the 4:4 product **C**, and a single TiO*C*Me$_3$ signal at 87 ppm (19 ppm downfield of HO*C*Me$_3$; cf. 84 ppm for TiO*C*HMe$_2$ with **D**, which was about 20 ppm downfield of HO*C*HMe$_2$). Again, wide spacings between the *Np* ^{1}H singlets and between their correlated ^{13}C peaks were consistent with bridging *Np* units, and the presence of a single set of signals from an unsymmetrical *Np* group indicated a symmetric dinuclear species, just as with **C**. The particularity of structure **E**, compared with the related **A**, is that the metal centers here are pentacoordinate, presumably because of steric congestion preventing further condensation or coordination of free alcohol. Indeed, the spectra showed no signs of metal-bound HO^{t}Bu, as the signals from liberated HO^{t}Bu were sharp and at normal positions.

Discussion

Ti(O^{i}Pr)$_4$ is tetrahedral and monomeric; steric congestion prevents its aggregation and the relief of that congestion drives its reactions. The simplest outcome of the reaction of H$_2$*Np* with 1 equiv of Ti(O^{i}Pr)$_4$ is a mononuclear, tetrahedral complex Ti*Np*(O^{i}Pr)$_2$, with vacant sites that could be occupied by HO^{i}Pr, despite the entropic cost. However, with two coordinated HO^{i}Pr units, hexacoordinate Ti*Np*(O^{i}Pr)$_2$-(HO^{i}Pr)$_2$ is even more congested than Ti(O^{i}Pr)$_4$, presenting four O^{i}Pr groups per metal at 90° bond angles. More reasonably, the pentacoordinate monoadduct Ti*Np*(O^{i}Pr)$_2$-(HO^{i}Pr) can form, and then it can dimerize through O^{i}Pr and/or *Np* bridges to afford hexacoordinate products. The crystalline 2:2 material **A** no doubt resulted from dimerization through two *Np* bridges (Figure 7). The 3:3 product **D** may well have formed by, first, an unsymmetrical dimerization through one *Np* bridge and one O^{i}Pr bridge, with sufficient stability in the resulting intermediate for it to persist until a third monomer formed the remaining bridges. In contrast, the fact that Ti(O^{t}Bu)$_4$ produced only the **A**-like dinuclear **E** suggests that HO^{t}Bu is too bulky to coordinate and that TiO^{t}Bu groups are too bulky to serve as bridges, and so this reaction only followed one path, that analogous to the upper path of Figure 7.

Condensations of this sort increase the degree of metal utilization, i.e., the number of metals per ligated oxygen, while reducing the total number of oxygens, including those from exogenous HO^{i}Pr, required to achieve coordinative saturation; this reduces steric congestion and increases universal entropy. This is reminiscent of the explanation put forth by Lehn et al.[34] for the selective formation of certain metal−ligand assemblies over other possibilities under self-

(34) Kraemer, R.; Lehn, J.-M.; Marquis-Rigault, A. *Proc. Natl. Acad. Sci. U.S.A.* **1993**, *90*, 5394−5398.

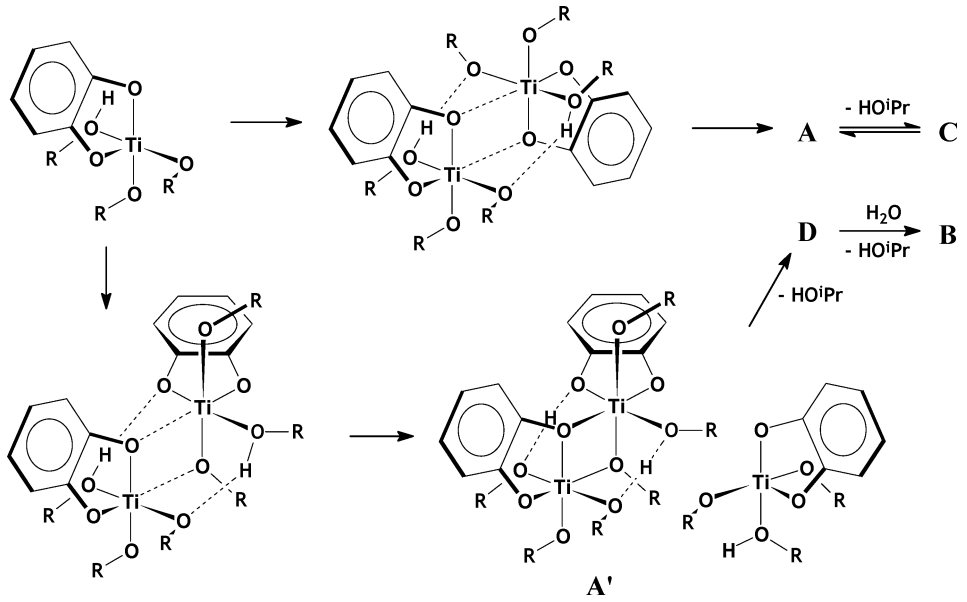

Figure 7. Possible modes of assembly of the observed condensation products: **A**/**C** by symmetrical coupling exclusively through *Np* bridges and asymmetric coupling through a mix of bridges in forming **D**, the putative precursor of **B**. For simplicity, *Np* ligands are depicted as catecholates.

assembly (equilibrating) conditions: the final outcome will have "maximum site occupancy", in the sense that it will maximally satisfy the coordination requirements of the metal centers while maximizing the use of the ligating atoms. Thus, hexacoordination in a mononuclear intermediate would require 6 oxygens, but only 5 are needed per Ti in **A**, 4 $^1/_2$ in **C**, and 4 $^1/_3$ in **D**. In the presence of limited amounts of water, further steric relief and further entropic gain can drive the formation of **B** (four O per Ti) from **D**. Moreover, the coordination of HO^{i}Pr is stabilized through hydrogen-bond bridges between metals in the multinuclear assemblies, but this is geometrically challenging when taking place on the same metal.

The **A**/**C** interchange (eq 1) was apparently an equilibrium (under thermodynamic control) governed by the availability of HO^{i}Pr and the crystal packing. Though "maximum site occupancy" would predict the minor product **D** to be marginally more stable than **C**, it was evidently very labile, but because they were observed both separately and together, **C** and **D** were not in equilibrium (through **A**). Hence, the reaction of the dinuclear precursor of **D** (**A′**) with the third metal center was probably irreversible, and the product distribution of eq 2 would have been established under kinetic control by the ratio of **A** to **A′** during the last step of the dimerization from their last common precursor.

The entropically favorable release of HO^{i}Pr in the condensation-aggregation of **A** to **C** is an evident driving force balancing against the crystal packing forces. Computations revealed a second, enthalpic driving force (Figure 8): Although they exaggerate the importance of hydrogen bonding, as evident when comparing the crystalline and computed structures of **A**, the computations nevertheless show an improved opportunity for hydrogen bonding in **D** and especially in **C**, as measured by the Ti−Ti and donor−acceptor (O−O) distances and by the O−H−O and trans O−Ti−O angles (Supporting Information). In both the chiral and the meso isomers (**C** and **C′**), there was a buckling of

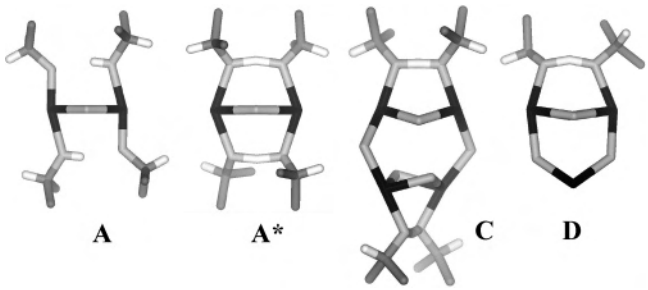

Figure 8. Depth-cued stick models of the cross-sections of crystalline **A** and of the ZINDO/1 structures of **A** (**A***), **C**, and **D**, showing the hydrogen-bonding and coordination geometries, with all but the bridging atoms omitted. Titanium atoms are black, oxygens are light gray, carbons are dark gray, and hydrogens are white.

the Ti_2O_2 rings and a reinforcement of the hydrogen bonding on the outer faces by compression of the participants. Even if exaggerated, this stronger binding would serve to preclude further condensation-oligomerization.

Though this study focused on H_2*Np*, it was noted at the outset that catechol itself gives the same reactions, and the analogue of **A** was recently described by Davidson et al.[6] The behavior of these enediols can be contrasted with that of other diols in their reactions with Ti(O^{i}Pr)$_4$. Saturated diols bearing side-chain groups, such as threitol or mannitol derivatives,[19,35] behave as divalent tridentates, displacing 2 equiv of HO^{i}Pr and causing dimerization of putatively pentacoordinate intermediates to achieve relatively stable hexacoordinate products of the same kind as **A**, that is, with the less-basic but less-encumbered alkoxide oxygens serving as bridges, but with additional coordination of the side-chain grouping instead of HO^{i}Pr. Less-basic diols, such as tartrate esters, are less-effective tridentates and in most cases behave as univalent or divalent bidentates in chelating to any one Ti atom, and stable hexacoordination is achieved with additional ligands.[15,36,37,3836−38] Enediols are strict bidentates,

(35) Bianchet, S.; Potvin, P. G. *Can. J. Chem.* **1992**, *70*, 2256−2265.

even less basic but less encumbered than tartrates, that require additional ligands (HO^iPr in the present cases) or aggregation, or both to achieve coordinative saturation.

Experimental Section

All reagents were Sigma-Aldrich products, while solvents were from Caledon Laboratories (Georgetown, ON, Canada) and were dried over activated 13X molecular sieves prior to use. $Ti(O^iPr)_4$ was distilled under Ar prior to use. $Ti(O^tBu)_4$ was purchased in Aldrich Sure-Seal bottles and used directly. NMR samples were prepared in $CDCl_3$ and sealed under Ar, and the spectra were acquired at 300 or 400 MHz on Bruker ARZ instruments, which made use of the standard Bruker pulse sequences. Mass spectra were obtained on a MALDI Voyager-DE spectrometer (PerSeptive Biosystems) equipped with a TOF detector in the positive ion mode. Crystal structure data collection, structural analysis, and refinement were carried out by Dr. Alan Lough at the University of Toronto. ZINDO/1 calculations were performed using *Hyperchem* (Hypercube, Gainesville, FL). Elemental analysis was carried out with weighing under N_2 by Guelph Chemical Laboratories, Guelph, ON, Canada.

Typical Procedure for Complex Formation. To a flame-dried, round-bottomed flask flushed with Ar and charged with 0−4 g of 13X molecular sieves was added H_2Np (0.3582 g, 2.24 mmol), which was then suspended in 3−4 mL of dried $CDCl_3$ with stirring. $Ti(O^iPr)_4$ (0.66 mL, 1 equiv) was added dropwise via a disposable syringe, producing a copious amount of yellow precipitate and a dark-red supernatant. A sample of the reaction mixture (0.5 mL) was transferred via syringe to a flame-dried, Ar-flushed NMR tube sealed with a septum.

($Ti Np(O^iPr)_2)_3(HO^iPr)$ (D). ^{1}H NMR (23 °C): δ 8.84 (s, 1H), 7.77 (s, 2H), 7.60 (m, 6H), 7.20 (m, 6H), 6.74 (2s, 4H), 5.39 (h, J = 8 Hz, 1H), 5.02 (h, J = 8 Hz, 2H), 4.80 (h, J = 8 Hz, 1H), 4.35 (br m, 2H), 4.16 (br m, ∼13H), 2.07 (br s, ∼11H, OH), 1.61 (d, J = 8 Hz, 6H), 1.44 (2d, J = 8 Hz, 12H), 1.34−1.17 (br d + d, ∼90H), 0.94 (d, J = 8 Hz, 6H) ppm. ^{13}C NMR (23 °C): δ 158.3, 155.23, 155.19, 130.3, 129.98, 129.95, 127.0, 126.6, 126.3, 123.6, 123.2, 122.7, 109.4, 106.8, 105.8, 84.2, 81.7, 80.4, 71.5 (br), 64.6 (br), 25.5−24.4 ppm. Samples prepared with 1 g of molecular sieves were nearly identical, differing only in the intensity of the HO^iPr signal near 4 ppm. Upon heating a sample containing both liquid and solid phases, the solids dissolved and a second set of signals assigned to **C** became apparent while the HO^iPr signal grew in relative intensity. Samples prepared with 2−4 g of molecular sieves were similar in appearance even at 23 °C, differing in the relative intensities of the two sets of signals, as well as that of the HO^iPr signal.

($Ti Np(O^tBu)_2)_2$ (E). Following the same procedure as for **D**, $Ti(O^tBu)_4$ (0.85 mL, 2.24 mmol) was used instead. A brownish precipitate was filtered through a glass frit under Ar to examine the reddish supernatant. ^{1}H NMR: δ 7.60 (m, 4H), 7.50 (s, 2H), 7.19 (m, 4H), 6.90 (s, 2H), 2.05 (br s, ∼15H), 1.54 (s, 36H), 1.29 (s, ∼135H) ppm. ^{13}C NMR: δ 155.9, 154.1, 130.0, 127.6, 125.7, 123.0, 121.9, 109.2, 105.3, 86.8, 68.1, 30.3, 30.2 ppm.

Crystallography. Diffraction intensities were collected on a Bruker-Nonius Kappa CCD instrument using a fine-focus sealed tube Mo Kα source and graphite monochromator. Unique reflections were corrected for absorption (*Denzo-SMN*) and used in all calculations. Heavy-atom positions were determined by direct methods (*SHELXS-97*). The remaining non-hydrogen atoms and hydrogen-bonding hydrogen atoms were located by difference Fourier maps, while the non-hydrogen-bonding hydrogen atoms were assigned idealized positions. Structure refinement used full-matrix least-squares on F^2 (*SHELXL-97*).

($Ti Np(O^iPr)_2)_2(HO^iPr)_2$ (A) and ($(Ti Np(O^iPr)_2)_2(HO^iPr))_2$ (C). A sample of the reaction mixture containing both liquid and solid phases was heated to dissolve the solids, then layered with an equal volume of dry petroleum ether under Ar. After 1 week, lightly reddish-orange crystals dotted with dark-red crystals were observed, and a light-colored one was removed and analyzed. Tables 1 and 2 list the important results. All but the hydrogen atoms were refined anisotropically. A hydrogen bond was found involving O(3) and O(5).

A separate batch of crystals from an identical sample was redissolved in dried $CDCl_3$ to give a reddish-orange solution containing material assigned to structure **C**. ^{1}H NMR: δ 7.66 (d, 4H), 7.39 (d, 4H), 7.23−7.07 (m + s, 12H), 6.44 (s, 4H), 5.35 (h, 4H), 5.03 (h, 2H), 4.12 (br h, ∼10H), 1.71 (d, 12H), 1.49 (d, 12H), 1.29 (h, 6H), 1.22 (2h, 6H+ ∼60H) ppm. ^{13}C NMR: δ 157.1, 156.5, 130.8, 129.4, 127.5, 126.4, 123.4, 123.0, 109.6, 105.9, 83.7, 79.0, 69.4 (br), 25.5−24.4 ppm.

To obtain an analytical sample of the lighter-colored material, the supernatant from another identical reaction mixture was carefully drawn off by syringe while under Ar. The remaining solid was rinsed with fresh $CDCl_3$, the solvent again drawn off before drying the residue under high vacuum and sealing. Anal. Calcd for $C_{38}H_{56}O_{10}Ti_2$ (**A**): C, 59.38; H, 7.34. Found: C, 58.79; H, 7.30.

$Ti_6Np_6O_4(O^iPr)_4(HO^iPr)_4\cdot 4CHCl_3$ (B). From the same sample that produced **A**, a second, dark-red crystal was also harvested and analyzed. Tables 1 and 3 list the important results. All H atoms were refined isotropically. Two disordered $CHCl_3$ solvate molecules were found with each half-cell. The non-hydrogen atoms at the major occupancy sites were refined anisotropically while those at minor sites were refined isotropically. In one case, the major and minor orientations shared a common Cl position, which was also refined isotropically. Two hydrogen bonds were found with each half-cell, designated O(9)−H(9O)−O(4) and O(11)−H(11O)−O(5).

Acknowledgment. We thank I. (Joanna) Vatavu for preparing the analytical sample of **A** and the Natural Sciences and Engineering Research Council of Canada for funding.

Supporting Information Available: Spectra in the presence of molecular sieves and at high temperature; detailed discussion of structure elucidation, molecular modeling, and mechanism of O^iPr-HO^iPr exchange; CIF file with crystallographic data. This material is available free of charge via the Internet at http://pubs.acs.org.

IC7013495

(36) Potvin, P. G.; Bianchet, S. *J. Org. Chem.* **1992**, *57*, 6629−6635.
(37) Potvin, P. G.; Fieldhouse, B. G. *Can. J. Chem.* **1995**, *73*, 401−413.
(38) Williams, I. D.; Pedersen, S. F.; Sharpless, K. B.; Lippard, S. J. *J. Am. Chem. Soc.* **1984**, *106*, 6430.